

## Construction of Zn<sup>II</sup>/Cd<sup>II</sup>-CPs and their fluorescent detection for Fe<sup>3+</sup>, Cr<sub>2</sub>O<sub>7</sub><sup>2-</sup> and TNP in water *via* luminescence quenching

Chaoxiong Li,<sup>a</sup> Xuancheng Sun,<sup>a</sup> Xianggao Meng,<sup>\*b</sup> Dunjia Wang<sup>a</sup> and Chunyang Zheng<sup>\*a</sup>

<sup>a</sup> Hubei Key Laboratory of Pollutant Analysis and Reuse Technology, College of Chemistry and Chemical Engineering, Hubei Normal University, Huangshi 435002, P. R. China.

<sup>b</sup> College of Chemistry, Central China Normal University, Wuhan 430079, P. R. China.

\* E-mail: [mengxianggao@ccnu.edu.cn](mailto:mengxianggao@ccnu.edu.cn); [cyzheng@hbnu.edu.cn](mailto:cyzheng@hbnu.edu.cn)

## CONTENTS

<b>Materials and methods.....</b>	S3
<b>Synthesis of ligand bmima.....</b>	S3
<b>Crystallographic studies.....</b>	S3
<b>Density functional theory (DFT) computations.....</b>	S3
<b>Fluorescence measurements.....</b>	S4
<b>Table S1 Selected bond lengths (Å) and angles (o) for CP 1–5.....</b>	S5
<b>Table S2. SHAPE analysis of the Zn<sup>II</sup> and Cd<sup>II</sup> ions in CP 1–5.....</b>	S6
<b>Fig. S1. ESI-MS of the ligand bmima .....</b>	S7
<b>Fig. S2. <sup>1</sup>H NMR spectra of bmima in CDCl<sub>3</sub>,.....</b>	S7
<b>Fig. S3. <sup>13</sup>C NMR spectra of bmima in CDCl<sub>3</sub> .....</b>	S7
<b>Fig. S4 IR spectra of complexes CP 1–5.....</b>	S8
<b>Fig. S5 PXRD patterns of CP 1–5.....</b>	S9
<b>Fig. S6 TGA curves of CP 1–5.....</b>	S10
<b>Fig. S7 Fluorescent emission spectra in solid state.....</b>	S11
<b>Fig. S8 Fluorescence spectra of CP 1 for sensing Fe<sup>3+</sup> cation .....</b>	S11
<b>Fig. S9 Fluorescence spectra of CP 3 for sensing Fe<sup>3+</sup> cation .....</b>	S11
<b>Fig. S10 Fluorescence spectra of CP 1 for sensing Cr<sub>2</sub>O<sub>7</sub><sup>2-</sup> anion .....</b>	S12
<b>Fig. S11 Fluorescence spectra of CP 3 for sensing Cr<sub>2</sub>O<sub>7</sub><sup>2-</sup> anion .....</b>	S12
<b>Fig. S12 Fluorescence spectra of CP 1 for sensing different phenols .....</b>	S12
<b>Fig. S13 Fluorescence spectra of t CP 3 for sensing different phenols .....</b>	S13
<b>Fig. S14 PXRD patterns of CP 1 after the detection of analytes .....</b>	S13
<b>Fig. S15 PXRD patterns of CP 3 after the detection of analytes .....</b>	S14
<b>Fig. S16 UV-vis spectra of analytes and Ex of CP 1 and CP 3.....</b>	S14
<b>Figure S17 IR spectra of CP 1 and CP 3 after sensing different analytes.....</b>	S15
<b>Table S3 Comparison of CP 1 and CP 3 with recent LCPs luminescent sensors for Fe<sup>3+</sup>.....</b>	S16
<b>Table S4 Comparison of CP 1 and CP 3 with recent LCPs luminescent sensors for Cr<sub>2</sub>O<sub>7</sub><sup>2-</sup>...</b>	S17
<b>Table S5 Comparison of CP 1 and CP 3 with recent LCPs luminescent sensors for TNP.....</b>	S18

<b>References.....</b>	S19
------------------------	-----

## Materials and methods

With the exception of bmima, all solvents and materials were purchased without any purification. The elemental analyses of C, H and N were carried out with a Perkin-Elmer 240C automatic analyzer. Powder X-ray diffraction (XRD) were performed on Bruker D8 Advanced diffractometer with Cu- $\text{K}\alpha$  radiation ( $\lambda = 1.54186 \text{ \AA}$ ). Thermogravimetric analysis was carried out with a NETZSCH STA 449F5 (TG/DTA) thermal analyzer under nitrogen flow. IR spectra of the two compounds were performed on a Bruker AXS TENSOR-27 FT-IR spectrometer (FTIR) with pressed KBr pellets in the range of 4000–400 cm<sup>-1</sup>. Fluorescence measurements were carried out on an F4700 (Hitachi) fluorescence spectrophotometer at room temperature. UV-vis absorption analysis was performed on a U-3010 spectrophotometer at room temperature. The <sup>1</sup>H and <sup>13</sup>C NMR spectra were recorded on Bruker AV 300 MHz spectrometers using CDCl<sub>3</sub> as the solvent. Chemical shifts are reported relative to tetramethylsilane TMS (internal standard), and chemical shifts are expressed in  $\delta$  (ppm). Mass spectra were measured on a LCQ Advantage MAX (ESI-MS).

## Synthesis of ligand bmima

Synthesis of 9,10-bis((2-methyl-1H-imidazol-1-yl)methyl)anthracene (bmima) A mixture of 2-methyl-1H-imidazole (3.4 g, 50 mmol), NaOH (2.0 g, 50 mmol) and DMF (80 mL) was heated at 60 °C for 1 h, then 9,10-bis(bromomethyl)anthracene (9.1 g, 25 mmol) was added. After stirring for 12 h at 60 °C, the mixture was poured into 200 mL water. A yellow residue was obtained after filtering. The crude product was further purified by flash chromatography  $V(\text{CH}_2\text{Cl}_2)/V(\text{CH}_3\text{OH}) = 20:1$ , and a yellow power was obtained (yield: 72%). ESI-MS: m/z = 366.9 ([M + H]<sup>+</sup>). <sup>1</sup>H NMR (CDCl<sub>3</sub>, 300 MHz):  $\delta = 2.74$  (s, 6H), 5.94 (s, 4H), 6.16 (s, 2H), 6.72 (s, 2H), 7.58–7.61 (m, 4H), 8.15–8.18 (m, 4H) ppm. <sup>13</sup>C NMR (CDCl<sub>3</sub>, 75.4 MHz):  $\delta = 13.70, 42.57, 118.35, 124.21, 126.94, 127.24, 127.54, 130.72, 144.16$  ppm. Yellow block crystals of bmima were obtained by recrystallization in the mixed solvent of CH<sub>2</sub>Cl<sub>2</sub> and CH<sub>3</sub>OH. The detailed crystal data and structure refinement parameters are shown in [Table 1](#).

## Crystallographic studies

Single-crystal X-ray diffraction data of CP **1–5** were collected on a Bruker APEX-II CCD or Rigaku XtaLAB Synergy-I with  $\omega$ -scan pattern and Mo-K $\alpha$  radiation ( $\lambda = 0.71073 \text{ \AA}$ ) or Cu K $\alpha$  radiation ( $\lambda = 1.54178 \text{ \AA}$ ) at RT. The diffraction profiles were integrated using the SAINT program.<sup>S1</sup> The structures were solved with direct methods (SHELX),<sup>S2, S3</sup> and refined by fullmatrix least squares on  $F^2$  using OLEX3,<sup>S4</sup> which utilizes the SHELXL-2018 module. The hydrogen atoms were placed geometrically. All non-hydrogen atoms were refined anisotropically. The H atoms were generated from the computed positions and subjected to isotropic refinement. The guest DMF molecules and water molecules are too disordered to be modeled properly. So the

diffuse electron densities resulting from these solvent molecules are removed by using the SQUEEZE routine of PLATON program to produce solvent-free diffraction intensities.<sup>S5</sup> The guest molecules were quantified through the thermogravimetric analyses and elemental analyses. The relevant crystallographic data are summarized in **Table 1**. The chosen bond lengths as well as angles are presented in **Table S2**.

A solvent mask was calculated and 688 electrons were found in a volume of 3172 Å<sup>3</sup> in 1 void per unit cell for CP **1**. This is consistent with the presence of 1[C<sub>3</sub>H<sub>7</sub>NO], 0.5[H<sub>2</sub>O] per formula unit which account for 640.0 electrons per unit cell.

A solvent mask was calculated and 684 electrons were found in a volume of 3432 Å<sup>3</sup> in 1 void per unit cell for CP **3**. This is consistent with the presence of 1[C<sub>3</sub>H<sub>7</sub>O], 1[H<sub>2</sub>O] per Formula Unit which account for 688 electrons per unit cell.

### Density functional theory (DFT) computations

Density functional theory (DFT) computations were the Gaussian16 program package. Geometry optimizations of CP **1** and CP **3** fragment were carried out in the liquid phase at (SMD)B<sub>3</sub>LYP-D<sub>3</sub>/SDD~6-311G(d,p) level. The SMD implicit solvent model3 with water as the solvent was used to include the solvation effects. The hybrid-B3LYP exchange-correlation functional combined with the D3 version of Grimme's dispersion were employed. The Stuttgart/Dresden relativistic effective core potential and the associated valence basis set (SDD) were applied for Cd, while the 6-311G(d,p) basis sets were used for C, H, O and N. Harmonic vibrational frequencies were calculated afterwards to confirm the obtained structures are real stationary points. During optimizations, the Cd<sup>2+</sup> cations, the N and C atoms were fixed according to Single-crystal X-ray diffraction data, while H atoms of the CP **1** and CP **2** fragment were allowed to relax.

### Fluorescence measurements

Well-ground powder of CP **1** or CP **3** (3 mg) was suspended in deionized H<sub>2</sub>O (3 mL) using ultrasound for 30 min. For each sensing experiment, a 0.2 M aqueous solution of M(NO<sub>3</sub>)<sub>n</sub> (M<sup>n+</sup> = K<sup>+</sup>, Na<sup>+</sup>, Zn<sup>2+</sup>, Cd<sup>2+</sup>, Mn<sup>2+</sup>, Hg<sup>2+</sup>, Ag<sup>+</sup>, Co<sup>2+</sup>, Ni<sup>2+</sup>, Mg<sup>2+</sup>, Cu<sup>2+</sup>, Pb<sup>2+</sup>, Al<sup>3+</sup>, Cr<sup>3+</sup>, Fe<sup>3+</sup>) solutions or Na<sub>x</sub>A(A<sup>-x</sup> = NO<sub>2</sub><sup>-</sup>, Br<sup>-</sup>, I<sup>-</sup>, Cl<sup>-</sup>, H<sub>2</sub>PO<sub>4</sub><sup>-</sup>, SO<sub>4</sub><sup>2-</sup>, NO<sub>3</sub><sup>-</sup>, WO<sub>4</sub><sup>2-</sup>, Ac<sup>-</sup>, SCN<sup>-</sup>, HPO<sub>4</sub><sup>2-</sup>, HCO<sub>3</sub><sup>-</sup>, CO<sub>3</sub><sup>2-</sup>, Cr<sub>2</sub>O<sub>7</sub><sup>2-</sup>) solutions was prepared and titrated into the suspension of CP **1** or CP **3** at ambient temperature. Then, the fluorescence emission intensities of different metal ions in the mixed solvent system were measured. The anti-jamming capability of CP **1** and CP **3** were verified by competitive experiments by adding various other cations or anions (0.2 mM) into CP **1**/CP **3** (3 mg) with a Fe<sup>3+</sup> or Cr<sub>2</sub>O<sub>7</sub><sup>2-</sup> (0.2 mM) suspension in 3 mL H<sub>2</sub>O after sonication.

**Table S1.** Selected bond distances ( $\text{\AA}$ ) and angles ( $^{\circ}$ ) for complexes CP 1–5

CP 1			
Cd1-O1	2.3297(12)	Cd1-O2	2.5564(14)
Cd1-O3 <sup>#1</sup>	2.4802(14)	Cd1-O4 <sup>#1</sup>	2.3596(13)
Cd1-O1w	2.3294(14)	Cd1-N1 <sup>#2</sup>	2.3809(14)
Cd1-N2 <sup>#2</sup>	2.3007(16)		
O1-Cd1-O2	53.13(4)	O1-Cd1-O3 <sup>#1</sup>	134.39(4)
O1-Cd1-O4 <sup>#1</sup>	80.90(5)	O1-Cd1-N1 <sup>#2</sup>	91.15(5)
O2-Cd1-O3 <sup>#1</sup>	170.44(4)	O2-Cd1-O4 <sup>#1</sup>	133.98(4)
O3 <sup>#1</sup> -Cd1-O4 <sup>#1</sup>	53.71(4)	N1-Cd1-O4	94.22(6)
Symmetry codes: #1: $x$ , $1-y$ , $-1/2+z$ #2: $-1+x$ , $y$ , $z$			
CP 2			
Zn1-O1	1.9392(19)	Zn1-N2	2.028(2)
Zn1-O4 <sup>#1</sup>	1.928(2)	Zn1-N4 <sup>#2</sup>	2.051(3)
O1-Zn1-N2	114.61(9)	O4 <sup>#2</sup> -Zn1-N4 <sup>#1</sup>	113.55(13)
O1-Zn1-N4 <sup>#1</sup>	91.71(12)	O4 <sup>#2</sup> -Zn1-O1	131.69(10)
O4 <sup>#2</sup> -Zn1-N2	100.02(9)	N(2)-Zn1-N4 <sup>#1</sup>	102.13(11)
Symmetry codes: #1 $-1/2+x$ , $+y$ , $3/2-z$			
CP 3			
Cd1-O2	2.2432(11)	Cd1-N1 <sup>#1</sup>	2.2986(12)
Cd1-O1	2.5541(12)		
O2-Cd1-O2 <sup>#1</sup>	147.73(8)	O2-Cd1-O1 <sup>#1</sup>	106.16(5)
O2-Cd1-O1	53.56(4)	O2-Cd1-N1 <sup>#1</sup>	85.06(4)
O1 <sup>#1</sup> -Cd1-O1	110.78(7)	N1 <sup>#1</sup> -Cd1-O1	91.03(5)
N1 <sup>#1</sup> -Cd1-O1 <sup>#1</sup>	136.64(4)	N1 <sup>#1</sup> Cd1-N1	98.01(6)
Symmetry codes: #1 $-x$ , $+y$ , $1/2-z$			
CP 4			
Zn1-O1	2.0438(15)	Zn1-O2 <sup>#1</sup>	2.0407(15)
Zn1-O3 <sup>#2</sup>	2.0819(14)	Zn1-O4 <sup>#3</sup>	2.0416(15)
Zn1-N2	2.0143(16)		
O1-Zn1-O3 <sup>#2</sup>	86.85(7)	O2 <sup>#1</sup> -Zn1-O1	156.95(6)
O2 <sup>#1</sup> -Zn1-O3 <sup>#2</sup>	88.74(7)	O(2)1   Zn(1)   O(4)3	88.13(7)
O4 <sup>#3</sup> -Zn1-O1	87.21(7)	O4 <sup>#3</sup> -Zn1-O3 <sup>#2</sup>	157.14(6)
N2-Zn1-O2 <sup>#1</sup>	97.03(7)	N2-Zn1-O1	106.00(7)
N2-Zn1-O4 <sup>#3</sup>	98.98(7)	N2-Zn1-O3 <sup>#2</sup>	103.88(6)
Symmetry codes: #1 $1/2-x$ , $1/2-y$ , $1-z$ ; #2 $+x$ , $-1/2+y$ , $1/2-z$ ; #3 $1/2-x$ , $1-y$ , $1/2+z$			
CP 5			
Cd1-O2 <sup>#1</sup>	2.242(4)	Cd1-O4 <sup>#2</sup>	2.224(4)
Cd1-O3 <sup>#3</sup>	2.275(3)	Cd1-N1	2.201(4)
Cd1-O1	2.227(3)		
O2 <sup>#1</sup> -Cd1-O3 <sup>#2</sup>	86.04(15)	O4 <sup>#3</sup> -Cd1-O2 <sup>#1</sup>	87.03(16)
O4 <sup>#3</sup> -Cd1-O3 <sup>#2</sup>	156.54(14)	O4 <sup>#3</sup> -Cd1-O1	88.15(17)
N1-Cd1-O2 <sup>#1</sup>	107.56(14)	N1-Cd1-O43	100.31(15)

N1-Cd1-O3 <sup>#2</sup>	103.15(14)	N1-Cd1-O1	96.23(14)
O1-Cd1-O2 <sup>#1</sup>	156.21(14)	O1-Cd1-O3 <sup>#2</sup>	89.21(15)
Symmetry codes: #1 3/2-x, 3/2-y, 2-z; #1 3/2-x, 2-y, -1/2+z; 3+x, -1/2+y, 5/2-z			

**Table S2.** SHAPE analysis of the Zn<sup>II</sup> and Cd<sup>II</sup> ions in CP **1–5**

name	ions	label	shape	symmetry	distortion( $\tau$ )
CP <b>1</b>	Cd1	HP-7	Heptagon	$D_{7h}$	32.715
		HPY-7	Hexagonal pyramid	$C_{6v}$	21.290
		PBPY-7	Pentagonal bipyramid	$D_{5h}$	<b>2.457</b>
		COC-7	Capped octahedron	$C_{3v}$	8.104
		CTPR-7	Capped trigonal prism	$C_{2v}$	6.114
		JPBPY-7	Johnson pentagonal bipyramid J13	$D_{5h}$	5.643
		JETPY-7	Johnson elongated triangular pyramid J7	$C_{3v}$	21.622
CP <b>2</b>	Zn1	SP-4	Square	$D_{4h}$	28.809
		T-4	Tetrahedron	$T_d$	<b>1.789</b>
		SS-4	Seesaw	$C_{2v}$	5.805
		vTBPY-	Vacant trigonal bipyramid	$C_{3v}$	3.141
		4			
CP <b>3</b>	Cd1	HP-6	Hexagon	$D_{6h}$	28.779
		PPY-6	Pentagonal pyramid	$C_{5v}$	15.770
		OC-6	Octahedron	$O_h$	12.219
		TPR-6	Trigonal prism	$D_{3h}$	<b>7.214</b>
		JPPY-6	Johnson pentagonal pyramid J2	$C_{5v}$	19.955
CP <b>4</b>	Zn1	PP-5	Pentagon	$D_{5h}$	30.468
		vOC-5	Vacant octahedron	$C_{4v}$	1.095
		TBPY-5	Trigonal bipyramid	$D_{3h}$	5.635
		SPY-5	Spherical square pyramid	$C_{4v}$	0.217
		JTBPY-5	Johnson trigonal bipyramid J12	$D_{3h}$	7.940
CP <b>5</b>	Cd1	PP-5	Pentagon	$D_{5h}$	30.402
		vOC-5	Vacant octahedron	$C_{4v}$	1.194
		TBPY-5	Trigonal bipyramid	$D_{3h}$	5.620
		SPY-5	Spherical square pyramid	$C_{4v}$	<b>0.236</b>
		JTBPY-5	Johnson trigonal bipyramid J12	$D_{3h}$	7.999

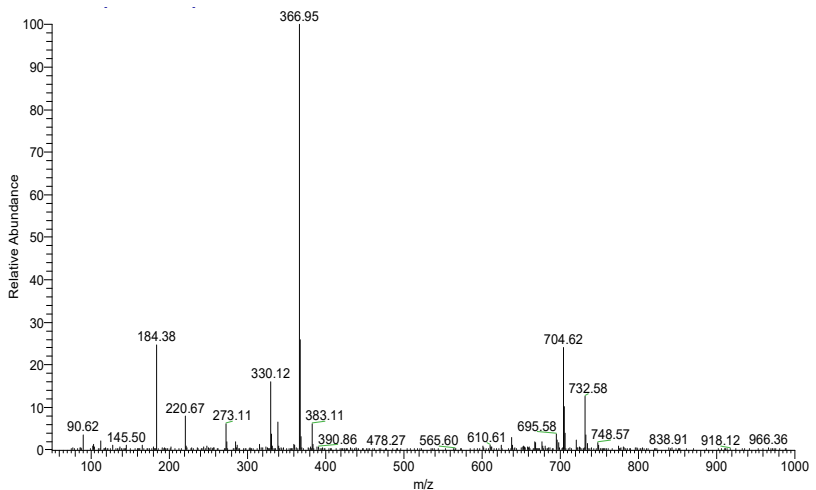


**Figure S1.** ESI-MS of the ligand bmima

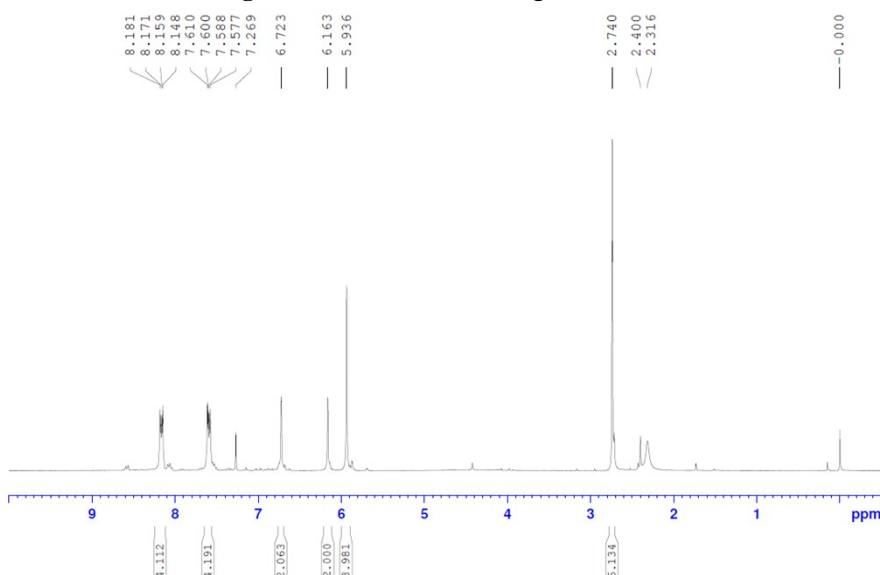


**Figure S2.** <sup>1</sup>H NMR spectra of bmima in CDCl<sub>3</sub>

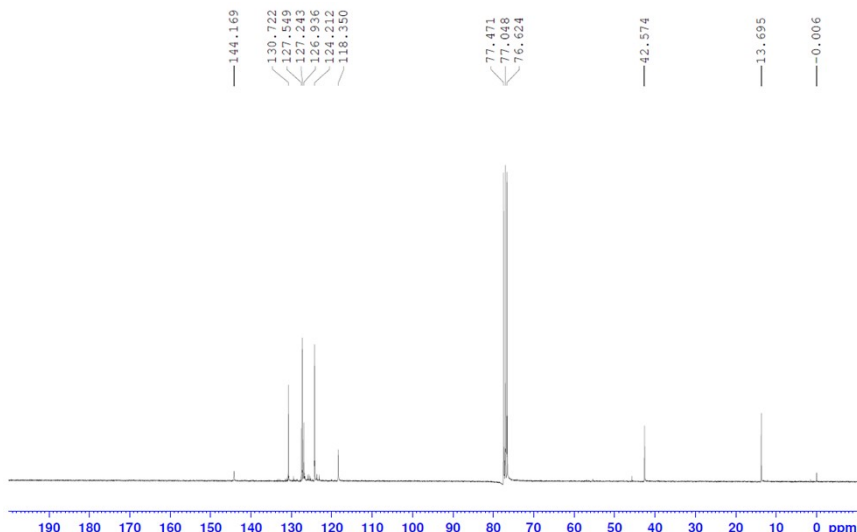


**Figure S3.** <sup>13</sup>C NMR spectra of bmima in CDCl<sub>3</sub>

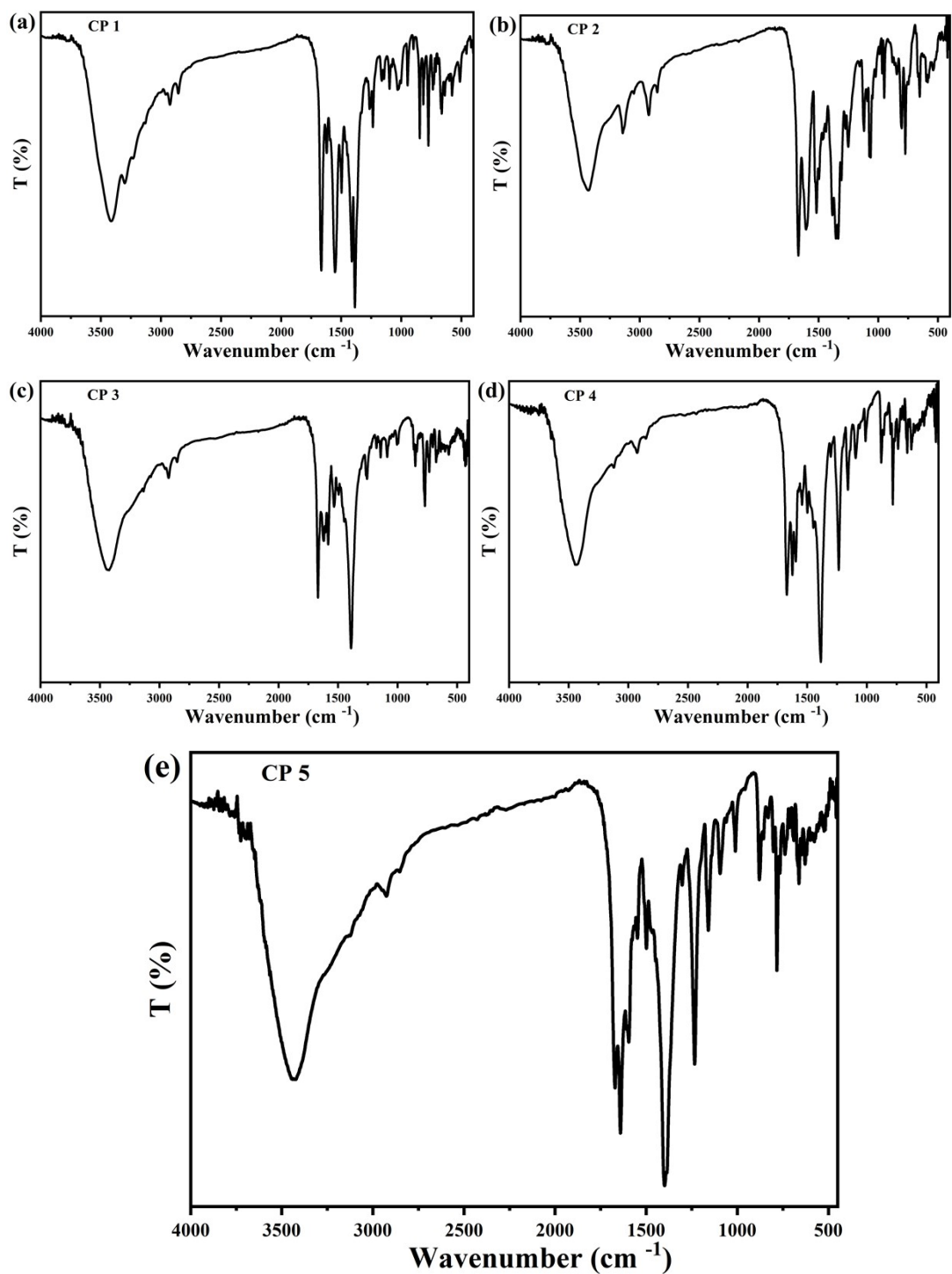


**Fig. S4** IR spectra of complexes CP 1–5

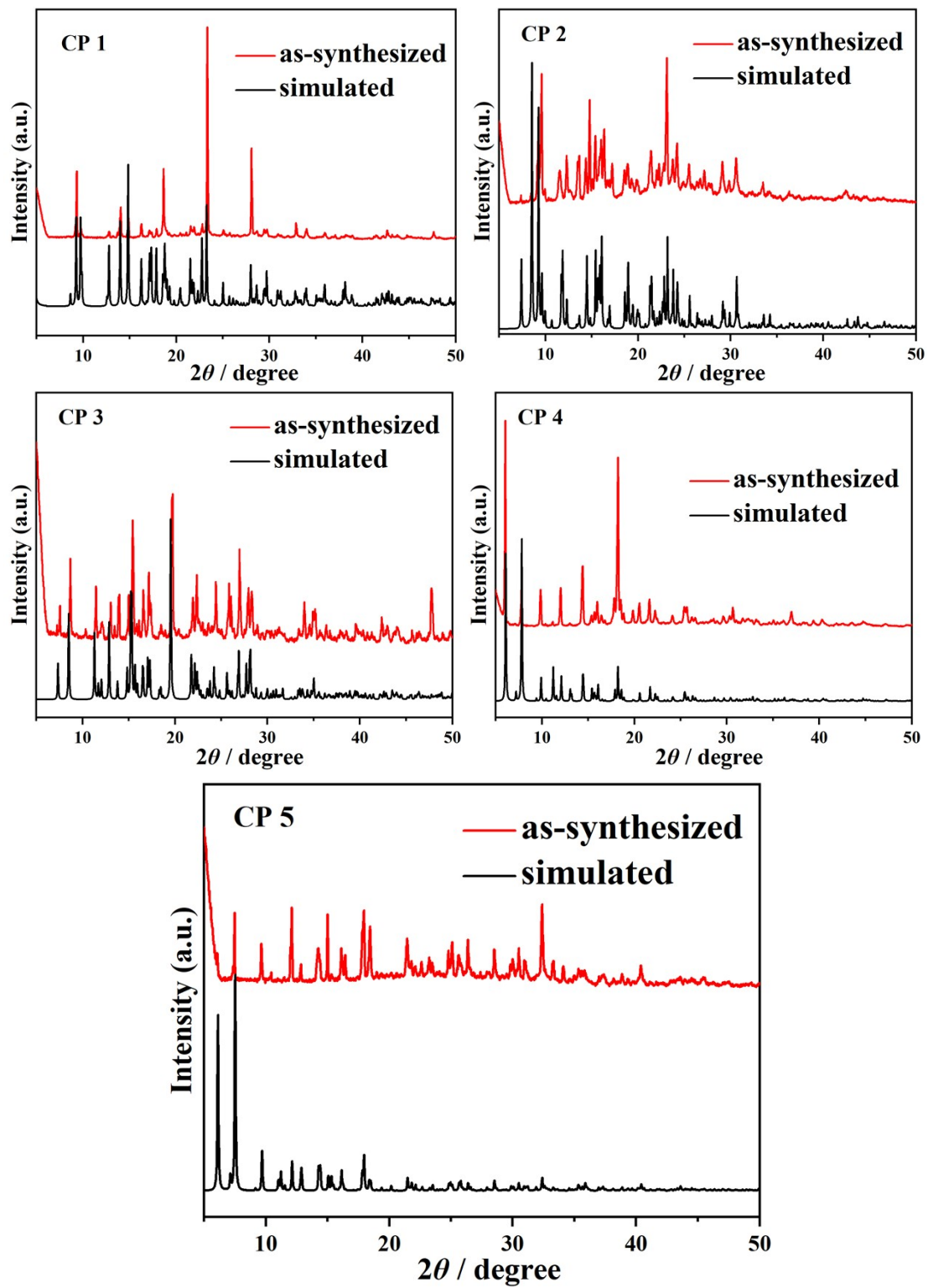
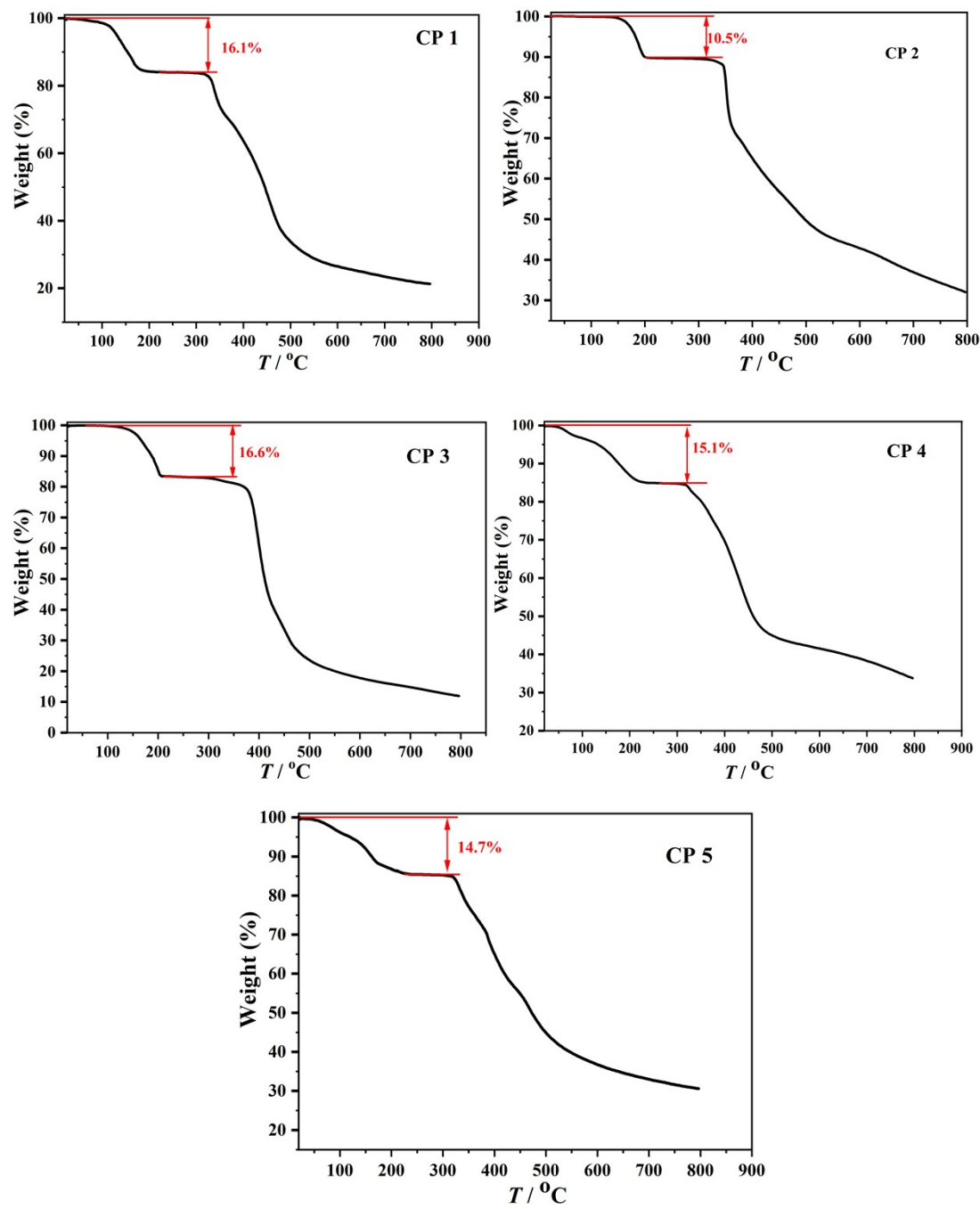
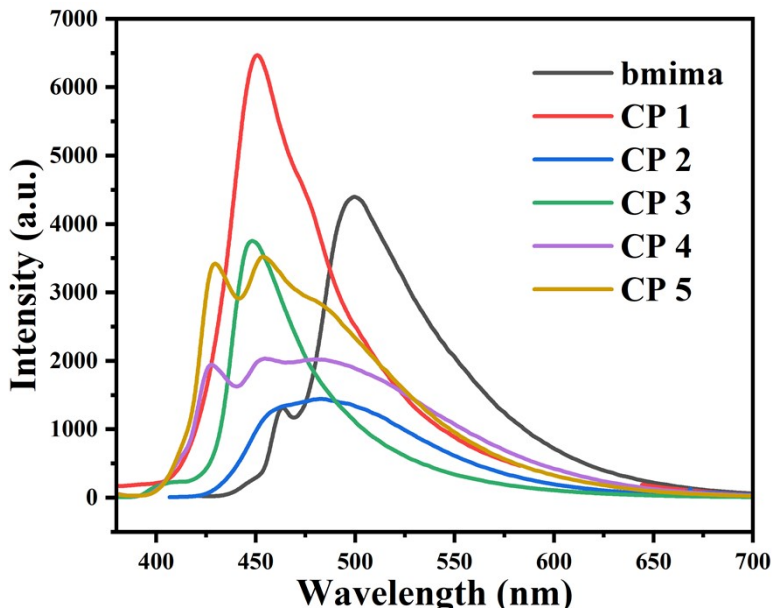


Fig. S5 PXRD patterns of CP 1–5



**Fig. S6** TGA curves of CP 1–5.



**Fig. S7** Fluorescent emission spectra of free ligand bmima and CP 1–5 in solid state at room temperature.

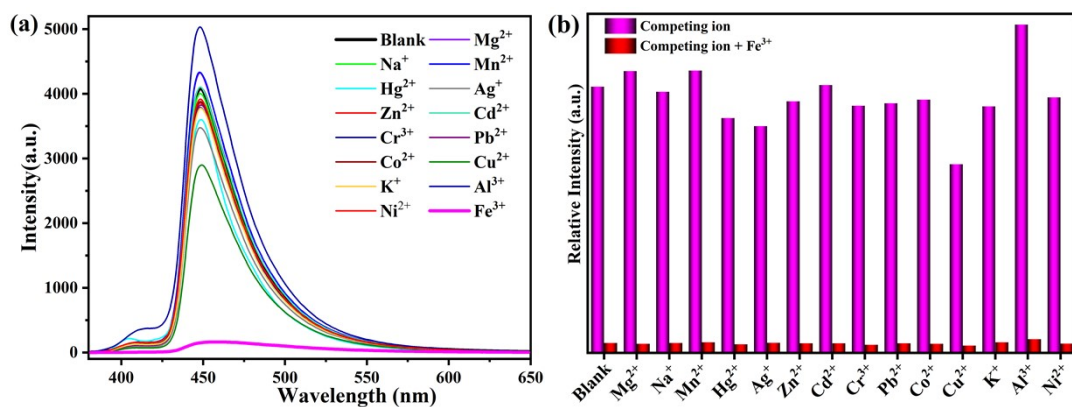


**Fig. S8** (a) Emission spectra of CP 1 dispersed in  $\text{H}_2\text{O}$  with the addition of different anions; (b) luminescence intensities of CP 1 before and after the addition of  $\text{Fe}^{3+}$  (0.2 mM) with the existence of mixed anions (0.2 mM).

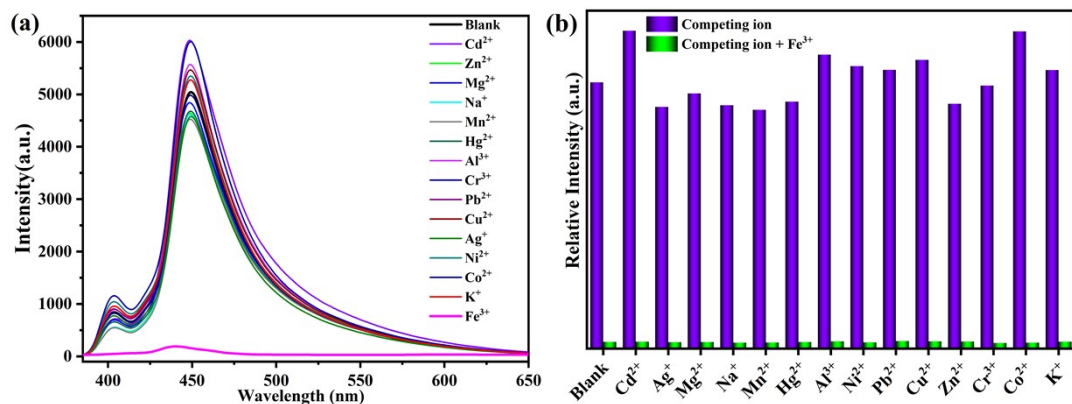


**Fig. S9** (a) Emission spectra of CP 3 dispersed in  $\text{H}_2\text{O}$  with the addition of different anions; (b) luminescence intensities of CP 3 before and after the addition of  $\text{Fe}^{3+}$  (0.2 mM) with the existence of mixed anions (0.2 mM).

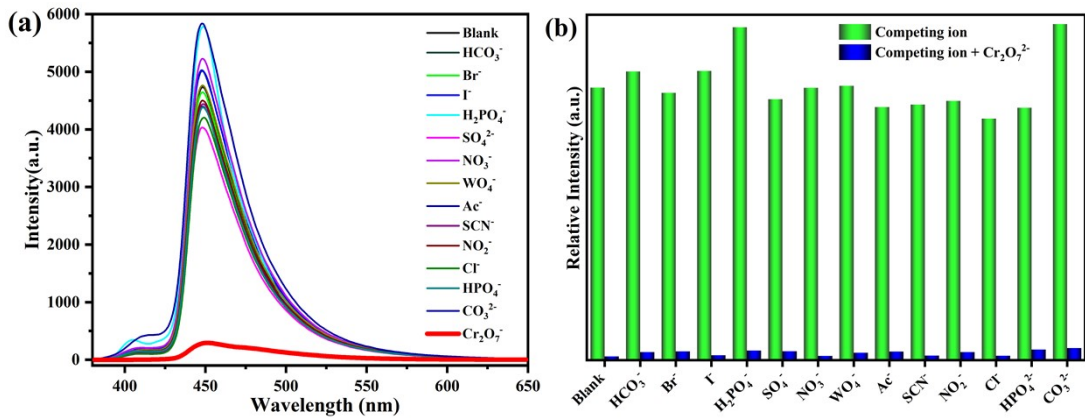


**Fig. S10** (a) Emission spectra of CP 1 dispersed in  $\text{H}_2\text{O}$  with the addition of different cations; (b) luminescence intensities of CP 1 before and after the addition of  $\text{Cr}_2\text{O}_7^{2-}$  (0.2 mM) with the existence of mixed cations (0.2 mM);

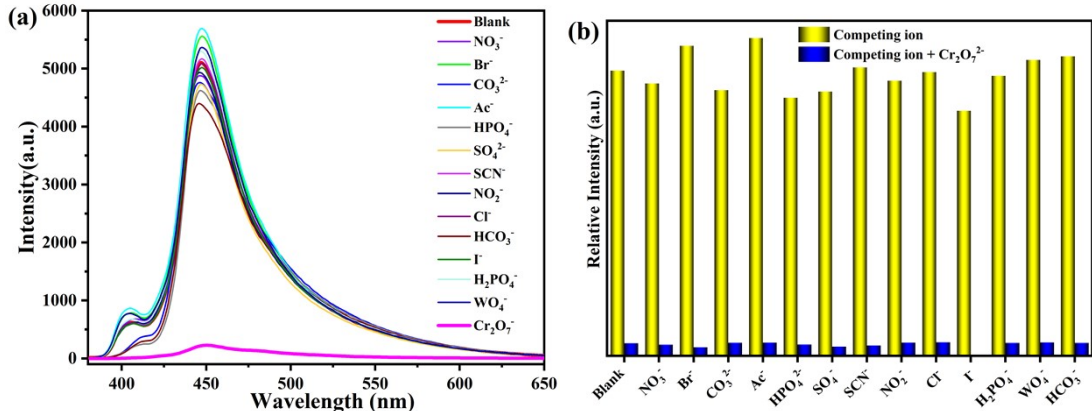


**Fig. S11** (a) Emission spectra of CP 3 dispersed in  $\text{H}_2\text{O}$  with the addition of different anions; (b) luminescence intensities of CP 3 before and after the addition of  $\text{Cr}_2\text{O}_7^{2-}$  (0.2 mM) with the existence of mixed anions (0.1 mM);

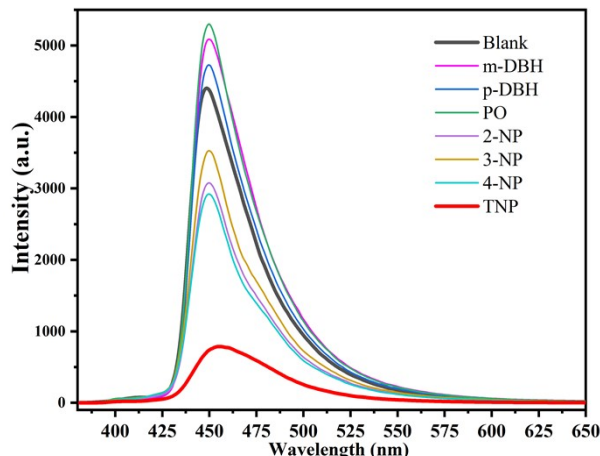


**Fig. S12** Fluorescence spectra (excited at 368 nm) of the suspension of CP 1 in 7 different phenols

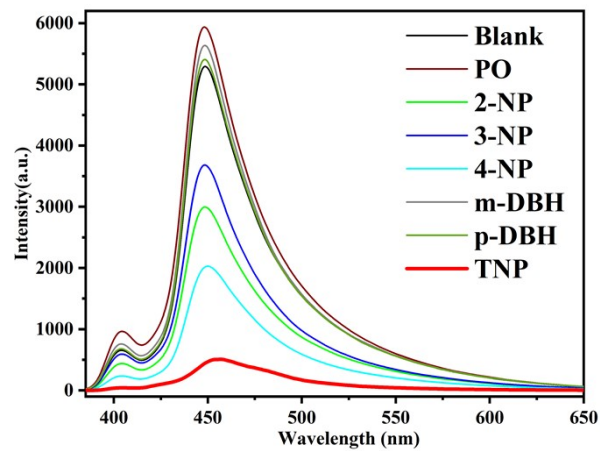


**Fig. S13** Fluorescence spectra (excited at 368 nm) of the suspension of CP 3 in 7 different phenols

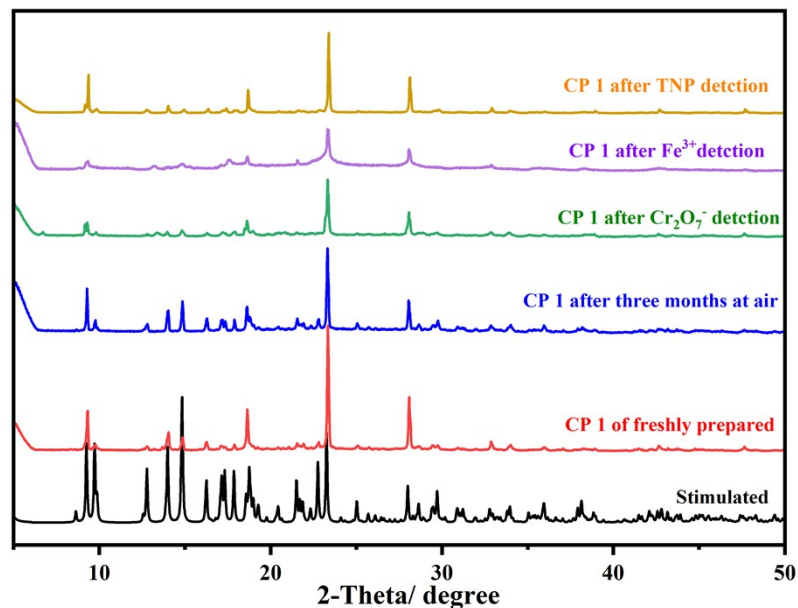


**Fig. S14** PXRD patterns of CP 1 after the detection of analytes

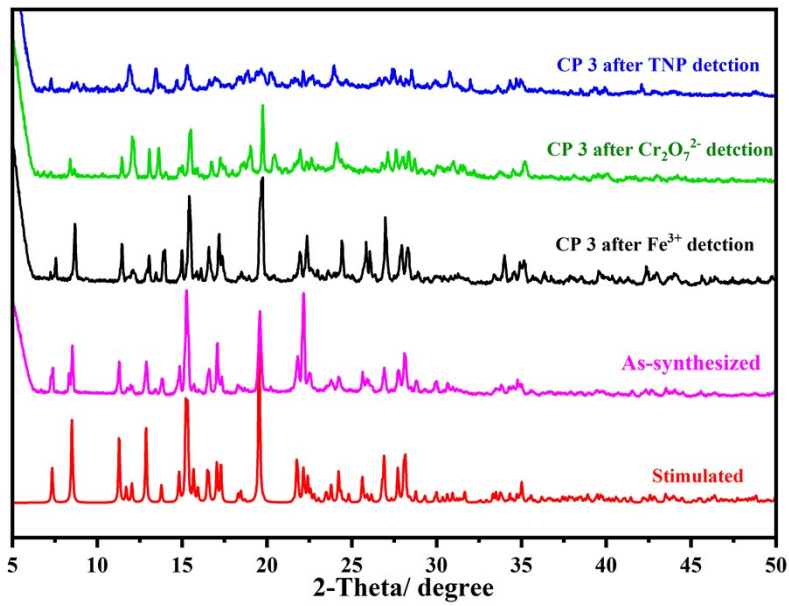


**Fig. S15** PXRD patterns of CP 3 after the detection of analytes

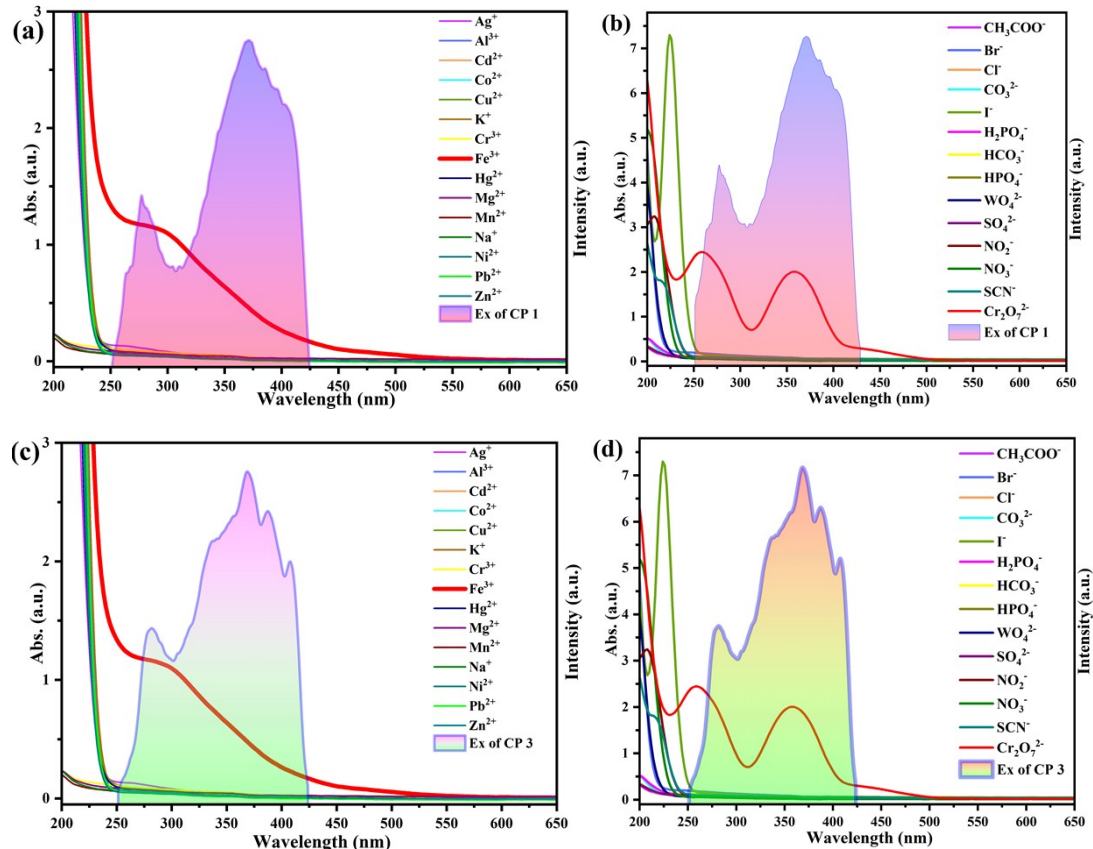


**Fig. S16** UV-vis spectra of different cations, anions and Ex of CP 1 (a, c), CP 3 (b, d) in water

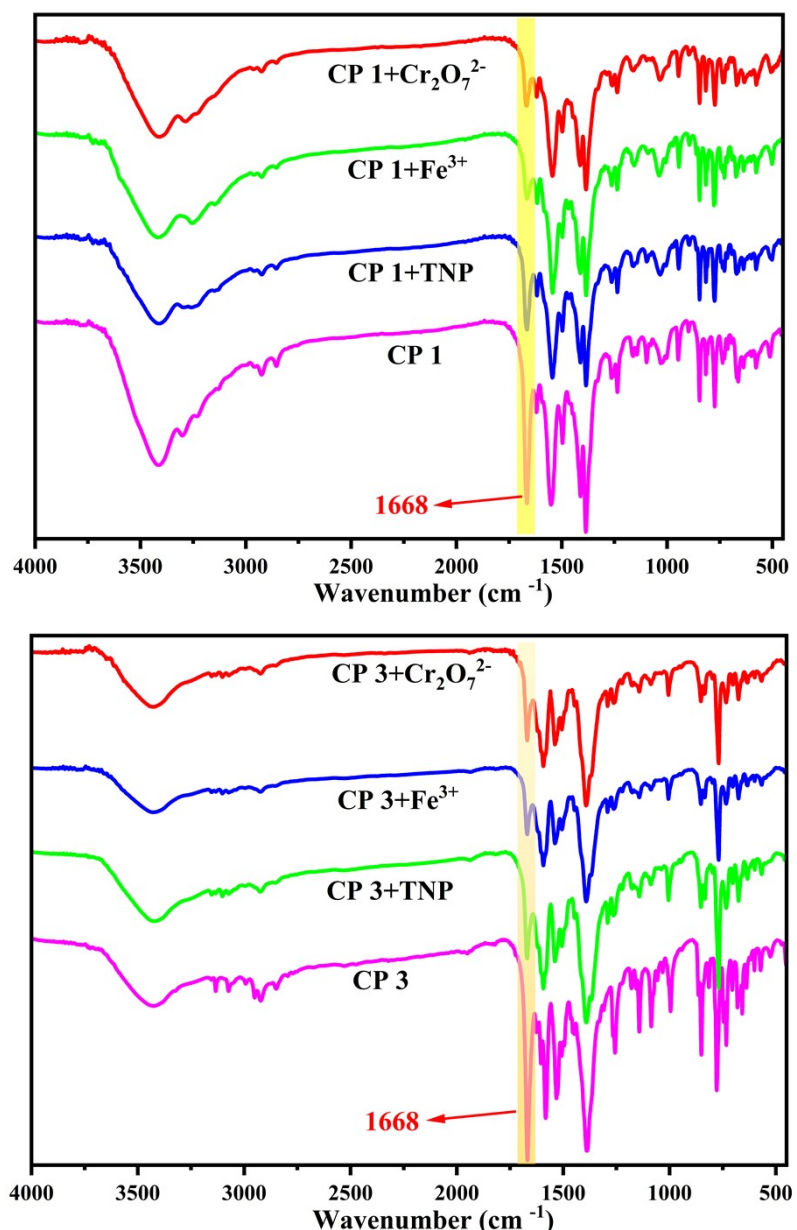


**Figure S17.** IR spectra of CP 1 and CP 3 after sensing different analytes at room temperature. The intensity at the  $1668 \text{ cm}^{-1}$  absorption band reduced after being soaked in the  $\text{H}_2\text{O}$  solution, and the change in the IR spectra is due to the DMF molecules gradually releasing after being soaked in the  $\text{H}_2\text{O}$  solution during the fluorescent sensing.

**Table S3** Comparison of CP **1** and CP **3** with recent LCPs-based luminescent sensors for Fe<sup>3+</sup>

LCPs-based chemosensor	<i>K</i> <sub>sv</sub> / M <sup>-1</sup>	LOD μM	Medium	Ref.
[Cd <sub>3</sub> (3-BABA) <sub>2</sub> (bpa) <sub>2</sub> ] <sub>n</sub>	1.14×10 <sup>4</sup>	0.539	H <sub>2</sub> O	S6
[Cd <sub>3</sub> (3-BABA) <sub>2</sub> (bpe) <sub>2</sub> ] <sub>n</sub>	2.98×10 <sup>4</sup>	0.265		
{[Cd <sub>3</sub> (3-BABA) <sub>2</sub> (bib)(DMA) <sub>2</sub> ]·H <sub>2</sub> O} <sub>n</sub>	0.805×10 <sup>4</sup>	0.748		
[Eu(BCB)(DMF)]·(DMF)1.5(H <sub>2</sub> O) <sub>2</sub>	4.7×10 <sup>4</sup>	0.415	H <sub>2</sub> O	S7
{[Zn(BIBT)(oba)]·DMA} <sub>n</sub>	3.27×10 <sup>4</sup>	0.056	EtOH	S8
{[Cd <sub>2</sub> (L)(1,4-NDC) <sub>2</sub> ]·EtOH}	1.94×10 <sup>4</sup>	NR	H <sub>2</sub> O	S9
{[Zn(L)-(dcdps)]} <sub>n</sub>	7.004×10 <sup>3</sup>	NR	H <sub>2</sub> O	S10
{Zn(L)(bdc)} <sub>n</sub>	9.066×10 <sup>3</sup>			
{Zn(L)(bdc)} <sub>n</sub>	4.984×10 <sup>3</sup>			
{[Cd(L)(bdc)·2H <sub>2</sub> O]·2DMF} <sub>n</sub>	6.387×10 <sup>3</sup>			
Cd-DTA	8.4×10 <sup>3</sup>	0.82	H <sub>2</sub> O	S11
Zn-DTA	6.24×10 <sup>3</sup>	1.07		
[Tb(tftba) <sub>1.5</sub> (phen)(H <sub>2</sub> O)] <sub>n</sub>	4.043×10 <sup>4</sup>	12.7	H <sub>2</sub> O	S12
[In <sub>5</sub> (TCA) <sub>2</sub> (HTCA) <sub>2</sub> (OH) <sub>5</sub> ]·6DMF·H <sub>2</sub> O	313907	0.382	H <sub>2</sub> O	S13
[Zn(H <sub>2</sub> L)(2,2-bipy)] <sub>n</sub>	1.61×10 <sup>4</sup>	0.708	H <sub>2</sub> O	S14
{[Eu(L <sub>2</sub> )(H <sub>2</sub> O)(DMF)]} <sub>n</sub>	3.10×10 <sup>4</sup>	1.57	H <sub>2</sub> O	S15
[Tb(L <sub>2</sub> )(H <sub>2</sub> O)(DMF)] <sub>n</sub>	2.89×10 <sup>4</sup>	0.91		
{[Cd(bmima) <sub>0.5</sub> (atp)(H <sub>2</sub> O)]·DMF·0.5H <sub>2</sub> O}	3.160×10 <sup>4</sup>	1.92	H <sub>2</sub> O	This work
{[Cd(bmima)(bpdc)]·2DMF}	2.674×10 <sup>4</sup>	2.96		

**Table S4** Comparison of CP **1** and CP **3** with recent LCPs-based luminescent sensors for Cr<sub>2</sub>O<sub>7</sub><sup>2-</sup>

LCPs -based chemosensor	K <sub>sv</sub> × 10 <sup>4</sup> /M <sup>-1</sup>	LOD μM	Medium	Ref.
[Zn <sub>2</sub> (OH)(1,4-ndc)1.5(Cz-3,6-bpy)]·2H <sub>2</sub> O	1.17	1.77	H <sub>2</sub> O	S16
{[Eu(L)(H <sub>2</sub> O)]·7H <sub>2</sub> O}	5.89	0.32		
{Tb(L)(H <sub>2</sub> O)}{Fan, 2023 #5} {Fan, 2021 #12} {An, 2022 #26}·7H <sub>2</sub> O}	3.26	0.57	H <sub>2</sub> O	S17
{[Cd(μ <sub>5</sub> -L)I] <sub>n</sub>	1.85	12.46	H <sub>2</sub> O	S18
[Zn <sup>1</sup> (L)(4,4'-bbibp)] <sub>n</sub>	10.8	0.28		
[Zn(L)(1,4-bimb)] <sub>n</sub>	7.40	0.41	H <sub>2</sub> O	S19
[Zn(L)(4,4'-bidpe)] <sub>n</sub>	8.11	0.37		
Zn-(PBBA)(H <sub>2</sub> O)]·3DMF·2H <sub>2</sub> O	1.2	4.2	H <sub>2</sub> O	S20
{[Zn(L) <sub>0.5</sub> (bpea)]·0.5H <sub>2</sub> O·0.5DMF}	1.65	1.42		
{[Zn-(L) <sub>0.5</sub> (ibpt)]·H <sub>2</sub> O·DMF} <sub>n</sub>	1.02	2.21	H <sub>2</sub> O	S21
[Zn(L1)hfdba] <sub>n</sub>	0.5029	0.33		
{[Zn(L <sub>2</sub> )(hfdba) <sub>2</sub> ]·2H <sub>2</sub> O} <sub>n</sub> .	1.3268	83.5	H <sub>2</sub> O	S22
[Zn(OBA) <sub>2</sub> (L <sub>1</sub> )·2DMA] <sub>n</sub>	1.897	2.37	H <sub>2</sub> O	S23
[Zn(ttb)(bdc) <sub>0.5</sub> ] <sub>n</sub>	6.67	0.10	H <sub>2</sub> O	S24
Cd <sub>3</sub> L(BTB) <sub>2</sub> ·2DMF	2.06	1.2		
(Cd <sub>3</sub> O <sub>2</sub> )LBTC	2.44	1.4	H <sub>2</sub> O	S25
[Zn(L)·2MeOH·H <sub>2</sub> O	0.118	2.95	H <sub>2</sub> O	S26
Zn <sub>2</sub> (tpeb)(bpdc) <sub>2</sub> ·0.5DMA·4H <sub>2</sub> O	1.122	1.04	H <sub>2</sub> O	S27
{[Zn <sub>3</sub> (mtrb) <sub>3</sub> (btc) <sub>2</sub> ]·3H <sub>2</sub> O} <sub>n</sub>	0.277	4.52	H <sub>2</sub> O	S28
{[Cd(bmima) <sub>0.5</sub> (atp)(H <sub>2</sub> O)]·DMF·0.5H <sub>2</sub> O}	3.417	1.82 μM	H <sub>2</sub> O	This work
{[Cd(bmima)(bpdc)]·2DMF}	3.394	2.54 μM	H <sub>2</sub> O	This work

**Table S5** Comparison of CP **1** and CP **3** with recent LCPs-based luminescent sensors for TNP

LCPs-based chemosensor	$K_{sv} / M^{-1}$	LOD	Medium	Ref.
[Zn(bpeb)(sda)]	$3.5 \times 10^4$	$2.0 \times 10^{-5}$ M	DMF	S29
[Zn(poly-bpeb)(sda)]	$4.1 \times 10^4$	$7.0 \times 10^{-6}$ M	DMF	
{[Zn <sub>2</sub> (L)(DMF) <sub>3</sub> ]·2DMF·2H <sub>2</sub> O}	$2.61 \times 10^4$	0.64 ppm	DMF	S30
{(Me <sub>2</sub> NH <sub>2</sub> )(Zn) <sub>2</sub> L(H <sub>2</sub> O)} <sub>n</sub>	$1.42 \times 10^4$	0.54 ppm	DMF	S31
[Zn(H <sub>2</sub> L)(2,2-bipy)] <sub>n</sub>	$1.67 \times 10^4$	8.82 mM	DMF	S14
[ZnL1(2,6-BIP)]·2H <sub>2</sub> O·DMF	$1.44 \times 10^4$	4.05 μM	DMF	S32
[CdL1(2,6-BIP)]	$1.48 \times 10^4$	3.94 μM		
[Zn <sub>2</sub> L2(2,6-BIP)]·DMF	$5.0 \times 10^4$	1.16 μM		
[CdL2(2,6-BIP)]·DMF	$5.31 \times 10^4$	1.10 μM		
{[Zn(L)(bpe)0.5]·DMF} <sub>n</sub>	$2.4 \times 10^4$	61.5 ppb	H <sub>2</sub> O	S33
{[Zn(BINDI) <sub>0.5</sub> (bpa) <sub>0.5</sub> (H <sub>2</sub> O)}·4H <sub>2</sub> O] <sub>n</sub>	$4.9 \times 10^4$	0.6 ppm	H <sub>2</sub> O	S34
{[Zn(BINDI)0.5(bpe)}·3H <sub>2</sub> O] <sub>n</sub>	$1.29 \times 10^4$	1.5 ppm		
{[Eu <sub>4</sub> (NO) <sub>5</sub> (μ <sub>3</sub> -OH) <sub>2</sub> Cl <sub>4</sub> (H <sub>2</sub> O)]·(NO <sub>3</sub> )·(H <sub>2</sub> O) <sub>5</sub> } <sub>n</sub>	$0.92 \times 10^3$	NR	H <sub>2</sub> O	S35
[Zn(L)]·2MeOH·H <sub>2</sub> O	$3.21 \times 10^4$	0.11 μM	DMF	S26
[(NH <sub>2</sub> (Me) <sub>2</sub> ) <sub>6</sub> [Tb <sub>3</sub> (TDPAT) <sub>2</sub> (μ <sub>2</sub> -O) <sub>1.5</sub> ]·3EtOH·7.5H <sub>2</sub> O	$1.77 \times 10^4$	2.39 mM	H <sub>2</sub> O	S36
[Cd <sub>3</sub> (H <sub>2</sub> O)(H <sub>3</sub> L) <sub>2</sub> (dia) <sub>2</sub> ]·4DMA·10H <sub>2</sub> O	$1.43 \times 10^5$	NR	H <sub>2</sub> O	S37
[Zn-(PBBA)(H <sub>2</sub> O)]·3DMF·2H <sub>2</sub> O	$4.4 \times 10^4$	1.0 μM	H <sub>2</sub> O	S38
{Zn <sub>2</sub> (tpt) <sub>2</sub> (tad) <sub>2</sub> ·H <sub>2</sub> O}	$7.8 \times 10^4$	2.56 μM	H <sub>2</sub> O	S39
{[Cd(bmima) <sub>0.5</sub> (atp)(H <sub>2</sub> O)]·DMF·0.5H <sub>2</sub> O}	$4.65 \times 10^4$	1.31 μM	H <sub>2</sub> O	This work
{[Cd(bmima)(bpdc)]·2DMF}	$4.65 \times 10^4$	2.03 μM		

## Reference

- S1. SAINT, Version 6.02a, Bruker AXS Inc, Madison, WI, 2002.
- S2. G. M. Sheldrick, SHELXT-Integrated Space-Group and Crystal-Structure Determination, *Acta Crystallogr., Sect. A: Found. Adv.*, 2015, **71**, 3-8.
- S3. 37 G. M. Sheldrick, Crystal Structure Refinement with SHELXL, *Acta Crystallogr., Sect. C: Struct. Chem.*, 2015, **71**, 3-8.
- S4. O. V. Dolomanov, L. J. Bourhis, R. J. Gildea, J. A. K. Howard and H. Puschmann, OLEX2: a Complete Structure Solution, Refinement and Analysis Program, *J. Appl. Crystallogr.*, 2009, **42**, 339-341.
- S5. A. L. Spek, *Acta Crystallogr., Sect. C: Struct. Chem.*, 2015, **71**, 9-18.
- S6. G.-M. Huang, S. Li, M.-X. Ma, S.-M. Li, W.-Q. Li, Q.-L. Ni, L.-C. Gui and X.-J. Wang, *CrystEngComm*, 2023, DOI: 10.1039/d3ce00007a.
- S7. M. Y. Zhang, F. Y. Yi, L. J. Liu, G. P. Yan, H. Liu and J. F. Guo, *Dalton Trans.*, 2021, **50**, 15593-15601.
- S8. S.-L. Yao, Y.-C. Xiong, X.-M. Tian, S.-J. Liu, H. Xu, T.-F. Zheng, J.-L. Chen and H.-R. Wen, *CrystEngComm*, 2021, **23**, 1898-1905.
- S9. X.-K. Yang, W.-T. Lee, J.-H. Hu and J.-D. Chen, *CrystEngComm*, 2021, **23**, 4486-4493.
- S10. F.-Y. Ge, G.-H. Sun, L. Meng, S.-S. Ren and H.-G. Zheng, *Cryst. Growth Des.*, 2019, **20**, 1898-1904.
- S11. L. Deng, Y. Zhang, D. Zhang, S. Jiao, J. Xu, K. Liu and L. Wang, *CrystEngComm*, 2019, **21**, 6056-6062.
- S12. H.-H. Yu, J.-Q. Chi, Z.-M. Su, X. Li, J. Sun, C. Zhou, X.-L. Hu and Q. Liu, *CrystEngComm*, 2020, **22**, 3638-3643.
- S13. H. Zhang, Z.-J. Ding, Y.-H. Luo, W.-Y. Geng, Z.-X. Wang and D.-E. Zhang, *CrystEngComm*, 2022, **24**, 667-673.
- S14. L.-N. Wang, Y.-H. Zhang, S. Jiang and Z.-Z. Liu, *CrystEngComm*, 2019, **21**, 4557-4567.
- S15. X. Mi, D. Sheng, Y. Yu, Y. Wang, L. Zhao, J. Lu, Y. Li, D. Li, J. Dou, J. Duan and S. Wang, *ACS Appl. Mater. Interfaces*, 2019, **11**, 7914-7926.
- S16. P.-M. Chuang and J.-Y. Wu, *CrystEngComm*, 2021, **23**, 5226-5240.
- S17. L. Duan, C. Zhang, P. Cen, X. Jin, C. Liang, J. Yang and X. Liu, *CrystEngComm*, 2020, **22**, 1695-1704.
- S18. T. T. Wang, J. Y. Liu, J. D. An, Y. F. Shi, Y. Y. Zhang, J. Z. Huo, Z. G. Huang, Y. Y. Liu and B. Ding, *Spectrochim Acta A Mol. Biomol. Spectrosc.*, 2021, **254**, 119655.
- S19. C. Fan, G. Huang, Z. Xing, J. Wang, Y. Pang, Q. Huang, S. Huang, Z. Zong and F. Guo, *CrystEngComm*, 2023, **25**, 593-600.
- S20. W. Liu, J. Qiao, J. Gu and Y. Liu, *Inorg. Chem.*, 2023, **62**, 1272-1278.

- S21. G. Xian, L. Wang, X. Wan, H. Yan, J. Cheng, Y. Chen, J. Lu, Y. Li, D. Li, J. Dou and S. Wang, *Inorg. Chem.*, 2022, **61**, 7238-7250.
- S22. S. C. Pal, D. Mukherjee and M. C. Das, *Inorg. Chem.*, 2022, **61**, 12396-12405.
- S23. H. M. Chai, J. L. Yan, G. Q. Zhang, J. X. Wang, Y. X. Ren and L. J. Gao, *Inorg. Chem.*, 2022, **61**, 7286-7295.
- S24. S. Gai, R. Fan, J. Zhang, J. Sun, P. Li, Z. Geng, X. Jiang, Y. Dong, J. Wang and Y. Yang, *Inorg. Chem.*, 2021, **60**, 10387-10397.
- S25. M. Fan, B. Sun, X. Li, Q. Pan, J. Sun, P. Ma and Z. Su, *Inorg. Chem.*, 2021, **60**, 9148-9156.
- S26. Q. Sun, K. Yang, W. Ma, L. Zhang and G. Yuan, *Inorg. Chem. Front.*, 2020, **7**, 4387-4395.
- S27. B. B. Rath and J. J. Vittal, *Inorg. Chem.*, 2020, **59**, 8818-8826.
- S28. Y. Q. Zhang, V. A. Blatov, T. R. Zheng, C. H. Yang, L. L. Qian, K. Li, B. L. Li and B. Wu, *Dalton Trans.*, 2018, **47**, 6189-6198.
- S29. X. Y. Zhang, S. M. Zhao, R. Li, Z. H. Xu, M. Y. Wang, Y. F. Jiang, K. Chen, Y. Zhao and W. Y. Sun, *Dalton Trans.*, 2021, **50**, 4408-4414.
- S30. J.-C. Jin, J. Wu, Y.-X. He, B.-H. Li, J.-Q. Liu, R. Prasad, A. Kumar and S. R. Batten, *CrystEngComm*, 2017, **19**, 6464-6472.
- S31. J. Wang, X.-R. Wu, J.-Q. Liu, B.-H. Li, A. Singh, A. Kumar and S. R. Batten, *CrystEngComm*, 2017, **19**, 3519-3525.
- S32. D. Wang, Z. Hu, S. Xu, D. Li, Q. Zhang, W. Ma, H. Zhou, J. Wu and Y. Tian, *Dalton Trans.*, 2019, **48**, 1900-1905.
- S33. X. Wang, M. Lei, T. Zhang, Q. Zhang, R. Zhang and M. Yang, *Dalton Trans.*, 2021, **50**, 3816-3824.
- S34. S. S. Dhankhar, N. Sharma and C. M. Nagaraja, *Inorg. Chem. Front.*, 2019, **6**, 1058-1067.
- S35. X. J. Zhang, F. Z. Su, D. M. Chen, Y. Peng, W. Y. Guo, C. S. Liu and M. Du, *Dalton Trans.*, 2019, **48**, 1843-1849.
- S36. Y. Xiao, B. Li, Z. X. You, Y. H. Xing, F. Y. Bai, L.-X. Sun and Z. Shi, *J. Mater. Chem. C*, 2021, **9**, 3193-3203.
- S37. Q. An, S. Bao, X. Li, J. Sun and Z. Su, *New J. Chem.*, 2022, **46**, 11377-11381.
- S38. W. Liu, J. Qiao, J. Gu and Y. Liu, *Inorg. Chem.*, 2023, **62**, 1272-1278.
- S39. X. Zhuang, X. Zhang, N. Zhang, Y. Wang, L. Zhao and Q. Yang, *Cryst. Growth Des.*, 2019, **19**, 5729-5736.